[redacted]

RES/FSCB 2018-02

Independent Assessment of In-Vessel Retention and Steam Explosion for the NuScale Small Modular Reactor

H. Esmaili
S. Campbell
J. Schaperow

September 2018

Fuel and Source Term Code Development Branch
Division of Systems Analysis
Office of Nuclear Regulatory Research
United States Nuclear Regulatory Commission

[redacted]

[redacted]

TABLE OF CONTENTS

[redacted]

[redacted]

LIST OF FIGURES

[redacted]

LIST OF TABLES

LIST OF ACRONYMS

BAF	Bottom of active fuel
CNV	Containment vessel
CVCS	Chemical and volume control system
DHRS	Decay heat removal system
ECCS	Emergency core cooling system
EVSE	Ex-vessel steam explosion
FSAR	Final safety analysis report
IVR	In-vessel retention
IVSE	In-vessel steam explosion
LHS	Latin hypercube samples
LOCA	Loss-of-coolant accident
LWR	Light water reactor
PDF	Probability density function
PWR	Pressurized water reactor
RPV	Reactor pressure vessel
RVV	Reactor vent valve
TAF	Top of active fuel

[redacted]

1.0 IN-VESSEL STEAM EXPLOSION (IVSE)

1.1 Objective and Approach

The objective of the independent confirmatory analysis was to confirm that the likelihood of containment upper head failure due to in-vessel steam explosion is small. The potential for the failure of the containment lower head was not assessed, because it is unlikely to lead to a large release due to fission product deposition in the reactor and containment and scrubbing in the reactor pool.

The mechanism postulated to cause containment upper head failure was an in-vessel steam explosion sending an energetic slug upwards through the RPV, contacting the upper head and launching it into the containment upper head. The mechanism has been called alpha-mode failure (U.S. NRC, 1975).

For the confirmatory analysis, the staff used the approach in NUREG/CR-5030 (U.S. NRC, 1989). NUREG/CR-5030 documents an approach for assessing the probability of steam-explosion-induced containment failure. NUREG/CR-5030 also implements the approach for a representative large LWR (a PWR) and provides results of the implementation. NUREG/CR-5030 contains four parts. Part I is the overall approach to the analysis and how the deterministic analysis in the subsequent parts are integrated to estimate the probability of containment upper head failure. Part II is deterministic analysis of premixing of the molten core debris in the RPV lower plenum water. Part III is a deterministic analysis of expansion and energy partition. Part IV is a deterministic analysis of impact mechanics, dissipation, and vessel head failure.

The staff performed its confirmatory analysis using the following steps:

1. The staff wrote a MATLAB program that implemented both the approach and the inputs for a large LWR from NUREG/CR-5030 using the probabilistic framework shown in Figure 1.1. The samples (10,000) were generated using the Latin Hypercube Sampling (LHS) technique from NUREG/CR-3624.
2. The staff ran the program to verify that the results were consistent with the results shown in NUREG/CR-5030.
3. The staff adjusted the input parameters to reflect design differences between the large LWR modeled in NUREG/CR-5030 and the NuScale design and reran the program. The staff's adjustments are described below for the input distribution ID-1 through ID-7 in Figure 1.1 (see the region enclosed in red since the other parameters are not applicable to the NuScale design).

[redacted]

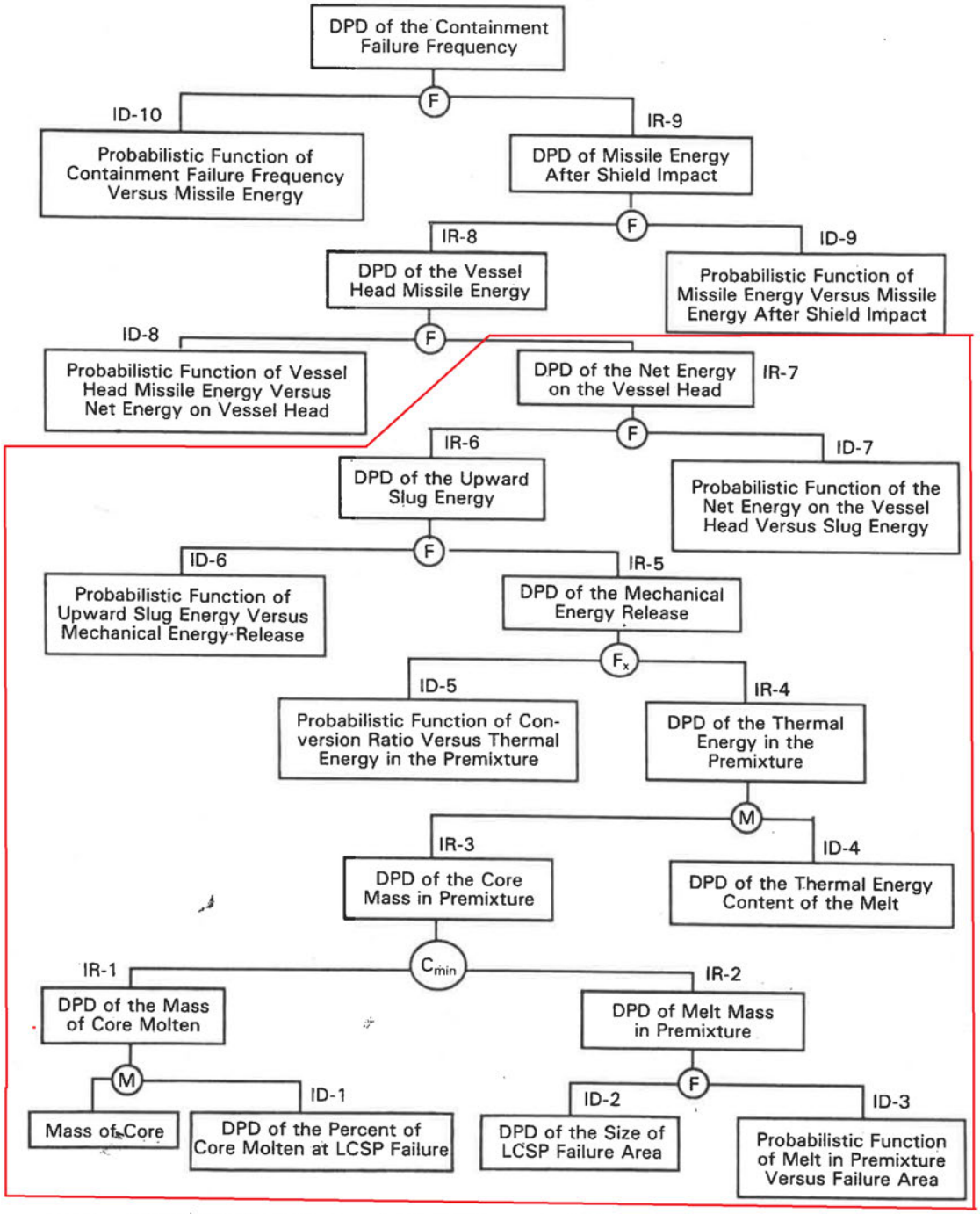

Fig. 1 Proposed probabilistic framework. The ID-*i* boxes refer to the various input distributions and the IR-*i* boxes to intermediate results. Operators are defined as follows: F_x = weighted function $[x \cdot F(x)]$, M = multiply, F = function, and C_{min} = compare.

Figure 1.1 Probabilistic framework for in-vessel steam explosion analysis

[redacted]

1.2 Boundary Conditions

ID-1 Fraction of core molten

For a large LWR, NUREG/CR-5030 used the following distribution for the fraction of core that is molten and available to pour into the lower plenum based on a 100-ton reactor core:

- Outside spectrum-of-reason result (probability level of 10^{-2}): 0.8-1
- Edge of spectrum result (probability level of 10^{-1}): 0.6-0.8
- Remaining result (remaining probability of 0.89): 0-0.6

Staff used the same probability distribution for ID-1 below; however, the resulting output distribution (IR-1 in Figure 1.1) is different for NuScale, since NuScale has a core of 12.5 tons consisting of both the fuel and cladding.

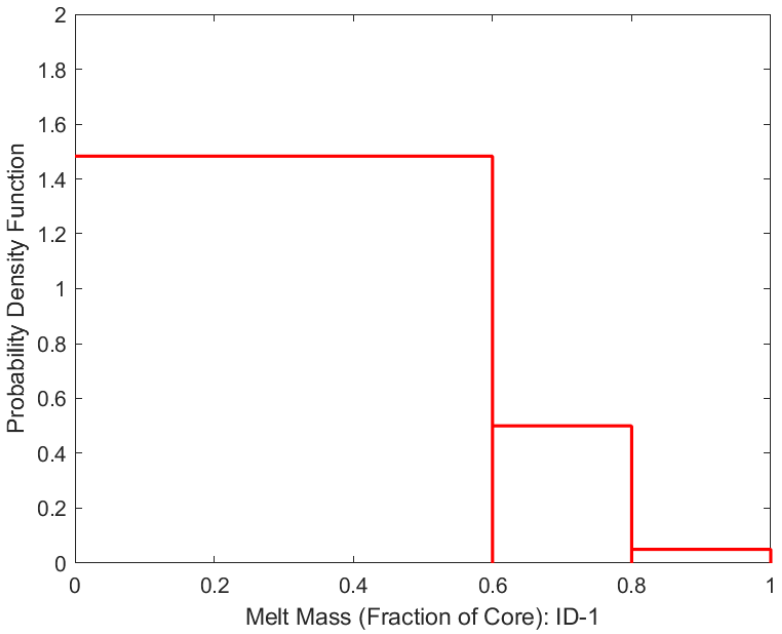

Figure 1.2 PDF for fraction of core molten (ID-1)

ID-2 Lower core plate failure area

For a large LWR with a lower core plate area of 10.5 m^2, NUREG/CR-5030 used the following distribution:

- Outside spectrum-of-reason result (probability level of 10^{-2}): 5.5 to 7.5 m^2
- Edge of spectrum result (probability level of 10^{-1}): 3.5 to 7.5 m^2
- Remaining result (remaining probability of 0.89): 0 to 3.5 m^2

[redacted]

[redacted]

NuScale has a lower core plate area of [redacted] m^2. Therefore, the staff used the following distribution (see Figure 1.3) to represent the NuScale design by scaling from the large LWR:

- Outside spectrum-of-reason result (probability level of 10^{-2}): [redacted] to [redacted] m^2
- Edge of spectrum result (probability level of 10^{-1}): [redacted] to [redacted] m^2
- Remaining result (remaining probability of 0.89): 0 to [redacted] m^2

Figure 1.3 PDF for lower core plate failure area (ID-2)

ID-3 Mass of core in pre-mixture

NUREG/CR-5030 Part II performed three alternative calculations to assess the mass of core in the pre-mixture. The 5% limit line was selected to represent the trend of the three calculations. The 95% limit line was selected to be a factor of two higher. A flat distribution was assumed between these two limit lines.

The staff used NuScale specific data with the first of the three alternative calculations in NUREG/CR-5030 (see equation below) to calculate the mass of core in the pre-mixture.

$$m_p = 2 * \rho_f * \delta * L * \text{square root of } (\pi * A)$$

The length was assumed to be [redacted] meters, which is the distance between the lower core plate and the inside bottom surface of the RPV. The staff used this calculation as the 5% limit line. The 95% limit line was selected to be a factor of two higher. A flat distribution was assumed between the two limit lines. These limits are shown by blue and red lines in the Figure 1.4.

[redacted]

[redacted]


[redacted]

Figure 1.4 Mass of core in pre-mixture (ID-3)

ID-4 Thermal energy of melt

The staff used the same thermal energy of melt as NUREG/CR-5030 (see Figure 1.5).

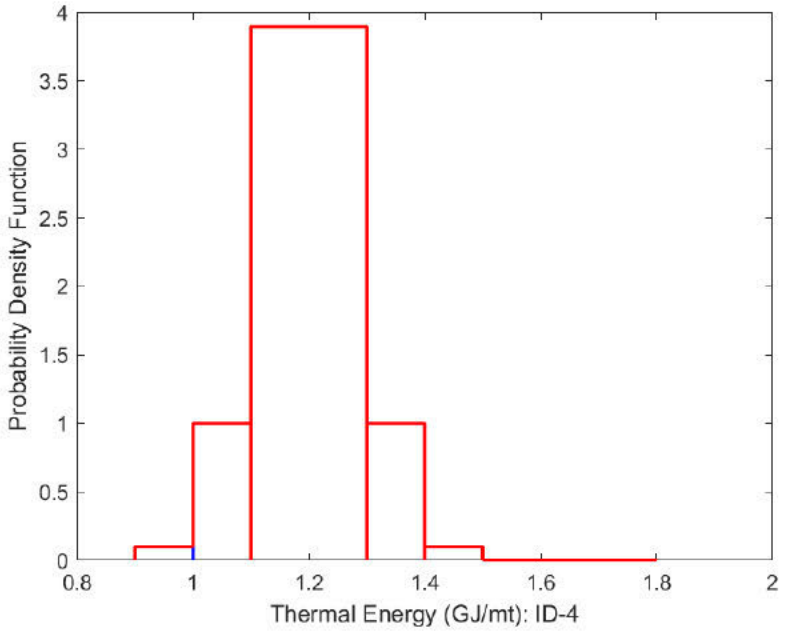

Figure 1.5 PDF of thermal energy of melt (ID-4)

[redacted]

[redacted]

ID-5 Conversion ratio

The staff used the same conversion ratio as NUREG/CR-5030. The 5% and 95% limits are shown by blue and red lines in the Figure 1.6. More recent analysis and experimental observations point to lower conversion ratios (typically < 5%) – see for example, (Liu, 2005) and (Corradini, Vapor Explosions in Light Water Reactors: A Review of Theory and Modeling, 1988). A sensitivity analysis was performed by assuming a lower bound of 5% for the conversion ratio and assuming an upper bound by a factor of 2 higher (a range of 0.05 to 0.1 at the 5% and 95% limit lines).

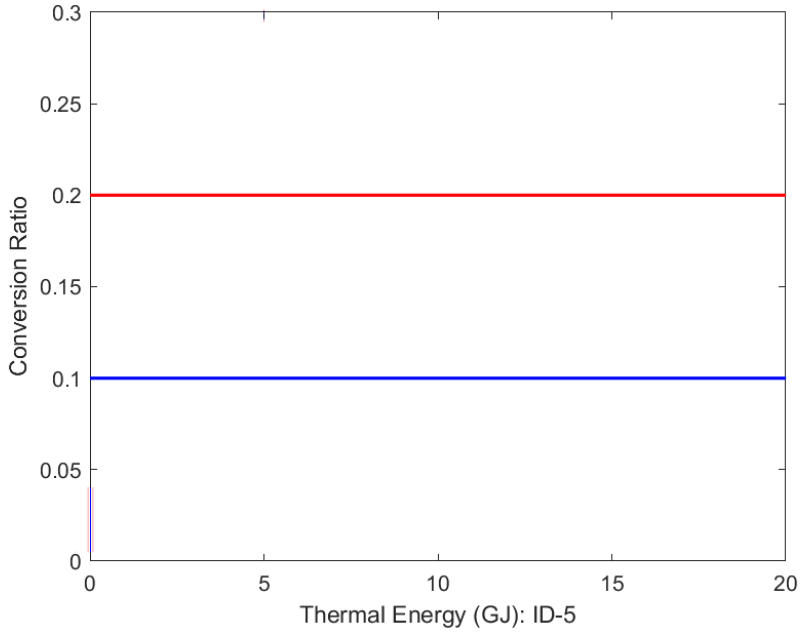

Figure 1.6 Conversion ratio (ID-5)

ID-6 Upward slug energy

NUREG/CR-5030 Part III performed thermodynamics analysis of the short-term expansion followed by the long term expansion in the lower plenum. The end of the short-term expansion is marked by the circumferential failure of the lower head. The analysis quantified the following energy losses:

- Upward flow in downcomer E_{dc}
- Structural deformation of lower head E_{sd}
- Sideways venting from circumferential break in lower head E_{bk}
- Downward motion of lower head E_{hm}

According to the analysis in (Corradini, Evaluation of Dynamic Pressures from Steam Explosions Applied to Advanced Light Water Reactors, 2011), the lower head of the NuScale RPV is unlikely to fail as a result of an in-vessel steam explosion. Therefore, the staff's confirmatory analysis only considered the first two of the above energy losses, namely, upward flow in the downcomer and structural deformation of the lower head.

[redacted]

[redacted]

The cases analyzed in NUREG/CR-5030 without lower head failure (those that just involved losses from upward flow in the downcomer and structural deformation of the lower head) are shown in the following table.

Table 1.1 Energy partitioning without lower head failure

Case	Mechanical energy release (MJ)	Upward slug energy (MJ)	Upward flow in downcomer (MJ)	Structural deformation of lower head (MJ)
EX2958	892	340	470	190
EX2950	414	54	195	90

A comparison of the downcomer and lower core plate flow areas for NUREG/CR-5030 and NuScale is shown in the following table. Because NuScale's ratio of downcomer area to lower core plate area is larger, NuScale's energy loss associated with upward flow in the downcomer is expected to be larger.

Table 1.2 Downcomer and lower core plate flow areas

	Downcomer flow area	Lower core plate area	Ratio of downcomer flow area to lower core plate area
Large LWR	3.5 m^2	10.5 m^2	0.33
NuScale	[redacted] m^2	[redacted] m^2	[redacted]

Because the energy losses are dominated by downcomer energy losses, NuScale is likely to have a higher ratio of upward slug energy to mechanical energy release compared with NUREG/CR-5030. Therefore, as a conservative representation for NuScale the staff used the ratio of upward slug energy to mechanical energy release from cases EX2958 and EX2950. The staff implemented these ratios as shown in NUREG/CR-5030 Part I Figure 33 (see Figure 1.7 below for NuScale).

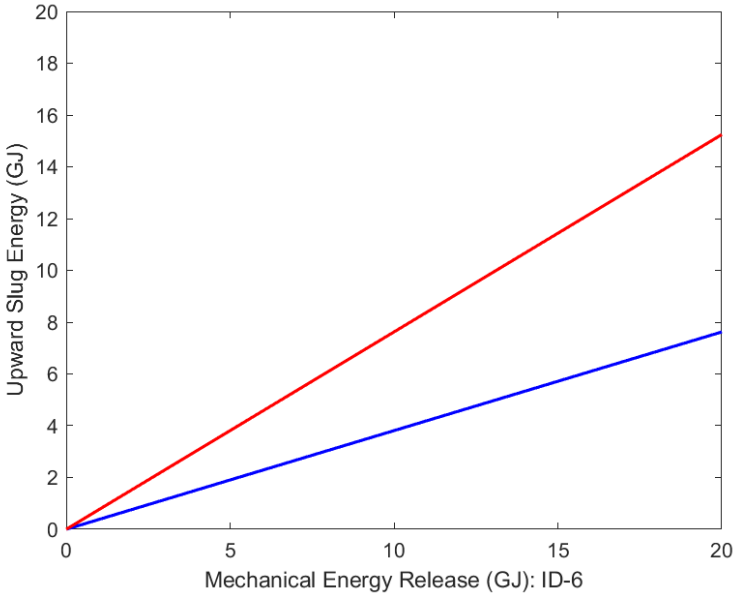

Figure 1.7 Upward slug energy (ID-6)

[redacted]

[redacted]

ID-7 Net energy in the upper heads after dissipation

NUREG/CR-5030 Part IV estimated energy losses as the slug moved up through the RPV and impacted the upper head as follows:

- Upper internals collapse (E_d^1 = 260 MJ) – experimentally determined
- Energy dissipation due to combined upper core support plate and core barrel deformations and radial slug expansion (E_d^2 = 0.34*(E_A-260) MJ)
- Upper core support plate failure (E_d^3 = 70 MJ) – calculated from shear blanking equation
- Head bolt failure (E_d^4 = 70-120 MJ)
- Direct head failure (E_d^4 = 140-195 MJ) – calculated from shear blanking equation

For NuScale, the staff used the results in NUREG/CR-5030 by scaling the energy reduction mechanisms. The material properties for NuScale RPV and containment upper heads (SA508) are similar to A533B used in NUREG/CR-5030 analysis.

E_d^1 = 50 MJ = 260 * 37/193 – scaled based on the number of assemblies

E_d^2 = 0.34*(E_A-50) MJ – the 0.34 factor is assumed to be the same

E_d^3 = 77 MJ – this includes the energy loss due to failure of the upper core support plate (35 MJ) and the pressurizer baffle plate (42 MJ). These dissipation energies were estimated from NUREG/CR-5030 by scaling the radius and the thickness of the plates using the shear blanking equation.

E_d^4 = 56-96 MJ – For direct head failure (circumferential tear of the RPV upper head followed by the failure of the CNV upper head), the staff estimated a range of dissipation energies using two methods: (1) shear blanking equation, and (2) a uniform stress distribution in the upper heads (i.e., (σ_U/2)*(ε_U/2)*(volume of head)) where σ_U is the ultimate tensile stress, ε_U is the total strain to failure assumed to be 0.21).

Combining the above dissipation energies, the expression for the net energy in the upper heads (E_o) is given by (see Figure 1.8):

E_o = max((0.66 E_i – 166),0) for the lower bound 5% (blue) limit line
E_o = max((0.66 E_i – 206),0) for the upper bound 95% (red) limit line

[redacted]

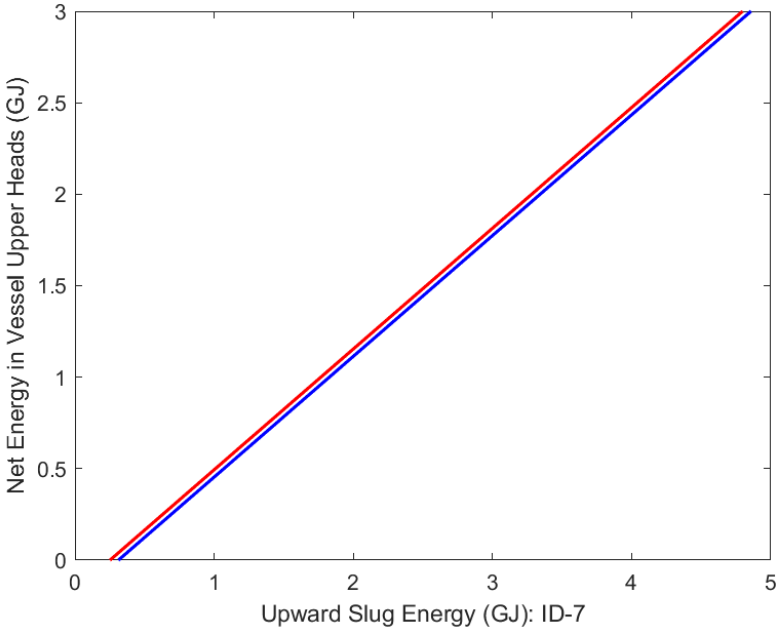

Figure 1.8 Net energy in upper heads after dissipation (ID-7)

1.3 Results

The 10000 samples were propagated through the probabilistic model in Figure 1.1, and the intermediate results are shown in Figure 1.9. The conditional probability of containment failure is about 4%. In the present analysis, some conservative assumptions were made including high conversion ratios associated with a thermodynamic model, neglect of venting after failure of the upper core plate, and the effects of the helical steam generator tubes. For example, reducing the conversion ratio from a range of 0.1-0.2 to 0.05 to 0.1 due to the fact the recent analysis suggest lower conversion ratios and the water in the lower plenum is saturated (thus reducing the explosion energetics) would reduce the conditional probability of containment failure to $5x10^{-4}$.

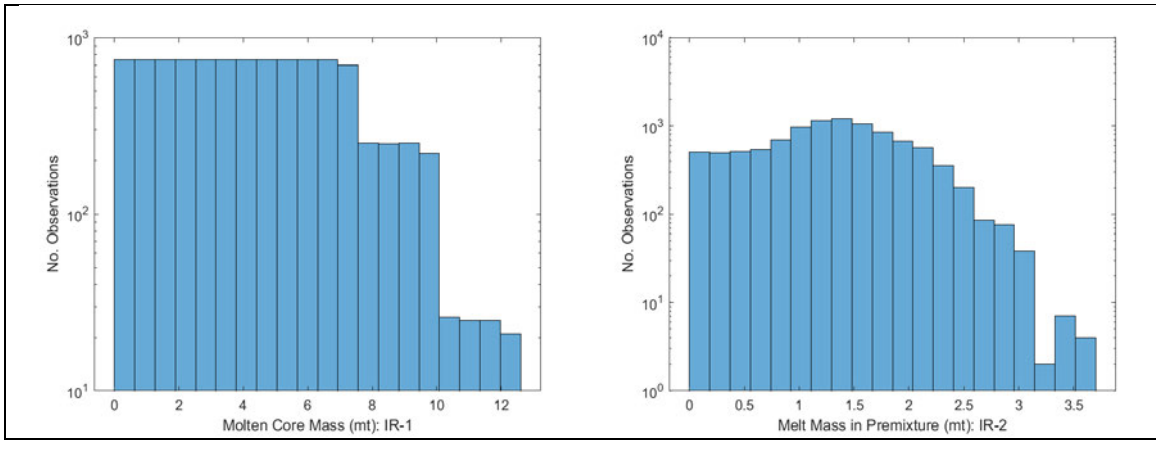

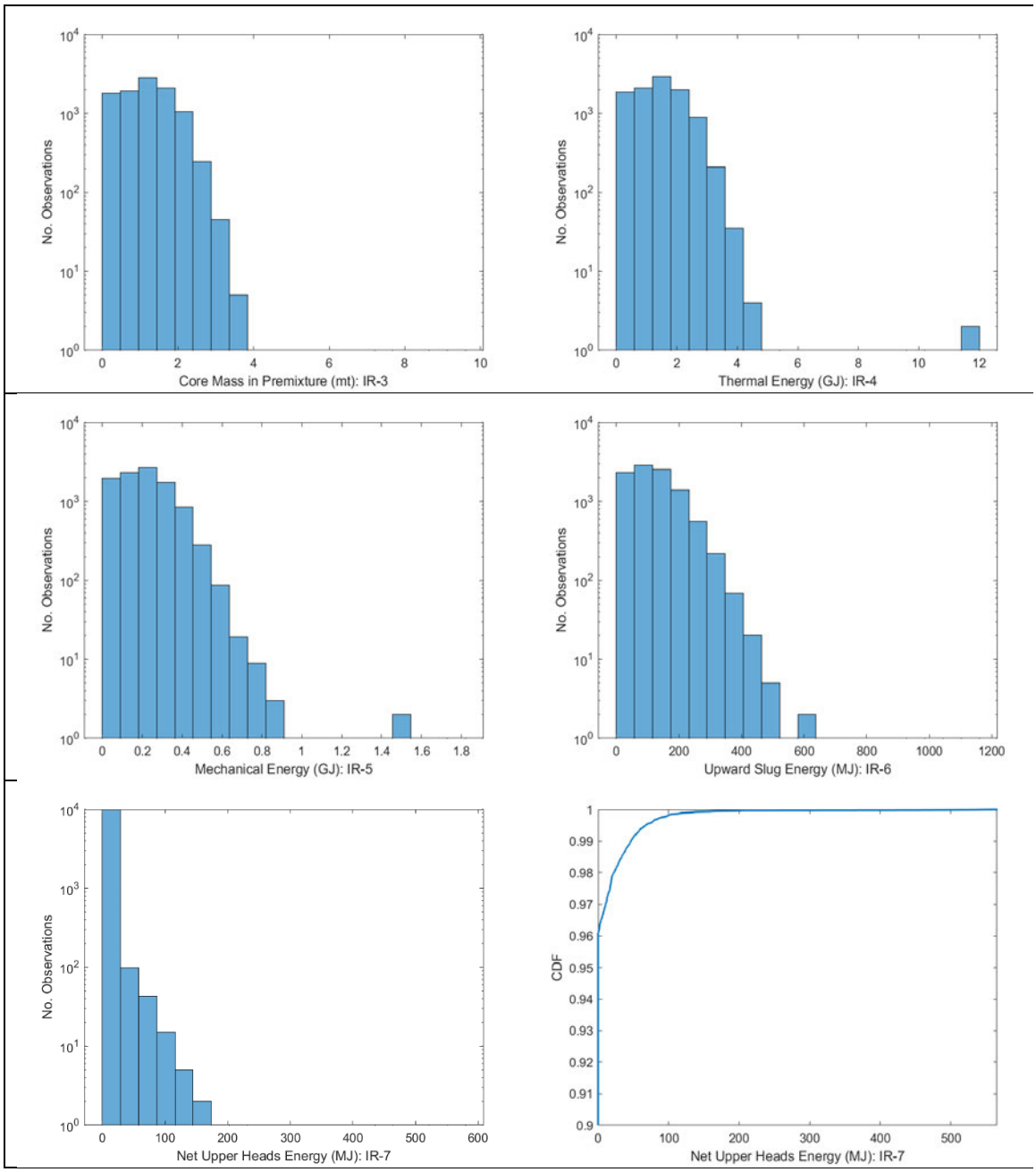

Figure 1.9 Results of in-vessel steam explosion analysis

[redacted]

2.0 IN-VESSEL RETENTION (IVR)

2.1 Objective and Approach

The objective of the independent confirmatory analysis was to explore the likelihood of RPV lower head failure following relocation of core to the lower plenum in the presence of external cooling provided by water inside the containment. The staff independent MELCOR confirmatory analysis documented in (U.S. NRC, 2018) (e.g., a scenario initiated by accidental opening of the reactor vent valve (RVV)) provided insights on the boundary conditions for the IVR analysis.

2.2 Boundary Conditions

The heat transfer mathematical model was taken from NUREG/CR-6849 (U.S. NRC, 2004) developed for the analysis of IVR in AP1000 and 1000 Latin Hypercube Samples were generated using the program in NUREG/CR-3624 (U.S. NRC, 1984). It should be noted that the present analysis ignores the presence of the alignment pin which can affect heat transfer at the bottom of the ceramic pool. But as will be shown later, the heat flux from the molten pool at the bottom is relatively low. The major concern is the focusing effect associated with formation of a metal layer on top of the ceramic pool.

The lower head inner and outer radii are [redacted] m and [redacted] m (lower head thickness of [redacted] m) with a core inventory of [redacted] kg of UO_2 and [redacted] of Zr according to the MELCOR model. The core contains about [redacted] kg of non-supporting structural steel and the lower core plate has a mass of [redacted] kg. For the initial conditions in the lower plenum, it is assumed that the mass of steel in the two layer configuration (a metal layer on top of a ceramic oxide layer) is directly proportional to mass of UO_2 relocated. The results of the MELCOR calculations indicate that rings 1 and 2 (23 assemblies or 62% of the core) relocate first and there is a possibility for the relocation of ring 3 which is the outer boundary ring. In the present analysis, the assumed distribution of the core UO_2 is shown in the Figure 2.1. A probability level of 10^{-1} is assumed for core relocation involving a major portion of the core (all the way to the entire core) while probability level of 10^{-2} is assumed for the core mass of 5,500 kg to 6,000 kg to account for the fact that the remaining probability level of 0.89 can represent the relocation of rings 1 and 2. The masses of Zr and ZrO_2 are calculated based on the fraction of the core oxidized as discussed in NUREG/CR-6894.

Depending on the scenario in the staff's independent MELCOR confirmatory analysis, the relocation of the core material can occur between 10 to 20 hours. The core decay powers at 10, 15, and 20 hours are used to develop the piecewise uniform probability distribution in Figure 2.2. In the LHS input model, 90 samples are taken between [redacted] MW range (corresponding to 15-20 hour relocation time) and 910 samples are assigned to [redacted] MW range (corresponding to 10-15 hour relocation time).

[redacted]

[redacted]


[redacted]

Figure 2.1 Distribution of UO_2 mass in the lower plenum for NuScale


[redacted]

Figure 2.2 Distribution of debris decay heat in the lower plenum for NuScale

[redacted]

[redacted]

2.3 Results

The distribution of the heat flux at three locations is shown in Figure 2.3. Staff calculations show that the heat flux at the bottom of ceramic (oxide) pool can vary between 78-95 kW/m^2 compared to 96-126 kW/m^2 at the top of the ceramic layer. The heat flux from the metallic layer varies between 255-520 kW/m^2.

According to the Revision 1 of the NuScale FSAR (page 19.2-16), "Conservative calculations, neglecting radiation from the top of the layer, determined the peak heat flux from the side of the layer is 618.3 kW/m^2, or a margin of about 50 percent. The peak heat flux for a best-estimate calculation with radiation included is only 175.5 kW/m^2. Thus, the focusing effect from a potential metallic layer above oxidic debris does not result in a challenge to RPV integrity." In addition, Revision 1 of the NuScale FSAR (page 19.2-15) estimates that the heat flux can range from 43 kW/m^2 at the bottom of the lower head to a maximum of 333 kW/m^2 at the RPV to alignment pin transition.

In general, the heat flux in the ceramic pool is lower than the applicant's analysis, and it is comparable in metal layer. In the present analysis, no attempt is made to quantify the probability of lower head failure due to uncertainties in the critical heat flux (i.e., lack of experimental data or equivalent analysis).

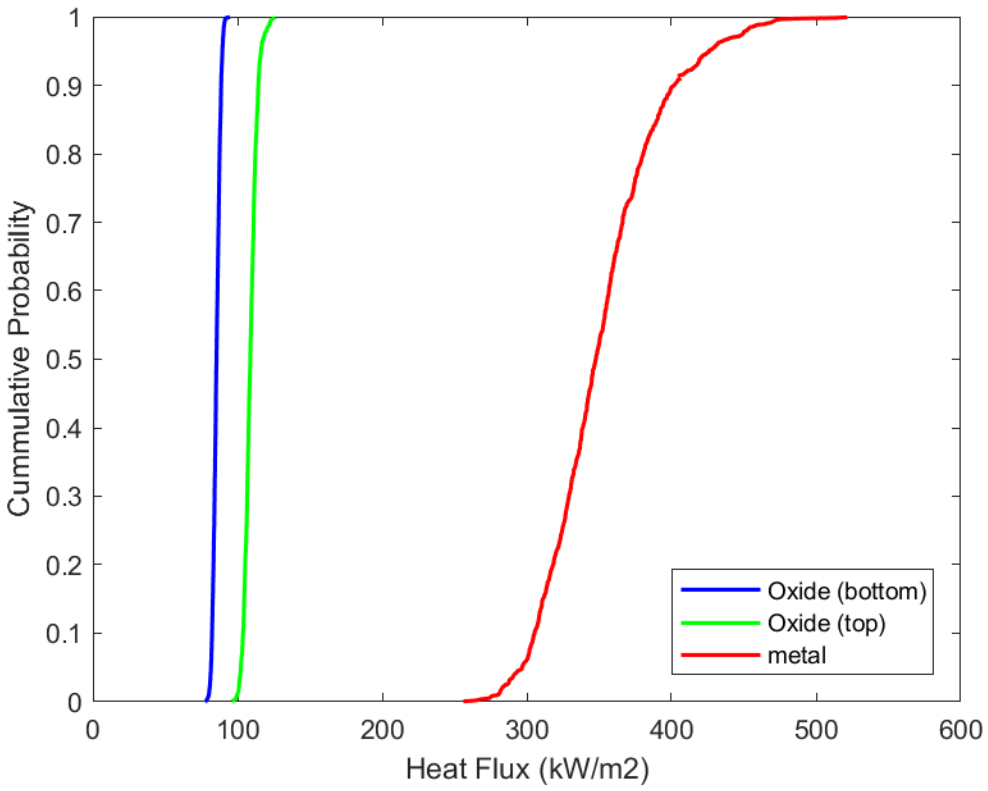

Figure 2.3 Distribution of heat flux in the ceramic and metallic layer

[redacted]

[redacted]

3.0 EX-VESSEL STEAM EXPLOSION (EVSE)

3.1 Objective and Approach

For scenarios with a LOCA into containment and ECCS failure, the RPV water is transferred to the containment as a result of the initial blowdown and subsequent boiloff from the RPV and condensation in the containment. As a result of loss of water from the RPV, the core heats up and is damaged. The corium subsequently relocates to the RPV lower plenum due to lower core plate failure. Corium that relocates to the lower plenum could form a molten pool and fail the RPV lower head.

Revision 1 of the NuScale FSAR includes an analysis to show that corium that relocates into the RPV lower plenum would be retained as a result of external cooling of the RPV by the water in the containment. Due to the phenomenological uncertainties in the retention of corium in the RPV, the staff assessed the potential for a steam explosion in the containment to cause a large release.

3.2 Results

As part of the staff's review of the applicant's analysis of severe accident mitigation, the staff performed independent confirmatory analysis with MELCOR for two scenarios involving LOCAs into containment. The staff's independent confirmatory analysis is documented in FSCB-18-01 (U.S. NRC, 2018).

In the first scenario (called LEC-06T in Revision 1 of the NuScale FSAR), it was assumed the LOCA was a stuck-open RVV. As a result of ECCS actuation, it was assumed that the other two RVVs subsequently opened. It also was assumed that the RRVs failed to open and the DHRS failed.

In the second scenario (called LCC-05T in Revision 1 of the NuScale FSAR), it was assumed the LOCA was a CVCS injection line break. As a result of ECCS actuation, it was assumed that the three RVVs subsequently opened. It also was assumed that the RRVs failed to open and the DHRS failed.

Figure 3.1 shows the staff's MELCOR predictions for LEC-06T containment water temperature and subcooling. Figures 3.2 and 3.3 show the staff's MELCOR predictions for LEC-06Tand LCC-05T for distribution of iodine. The figures show the amount of iodine in the RCS, in the containment, and remaining in the fuel. The figures also show the amount of iodine airborne in the RCS and in the containment.

Revision 1 of the NuScale FSAR Section 19.1.4.2.1.4 gives a criterion for large release of 2.9% of the core inventory of iodine. As shown in Figures 3.2 and 3.3, the amount of iodine airborne in the RPV and in the containment following lower core plate failure is less than 2.9% of the core inventory of iodine. Most of the iodine has deposited in the RPV and containment or remains in fuel. Therefore, a postulated failure of the containment above the reactor pool that is induced by an ex-vessel steam explosion is unlikely to cause a large release. Postulated failure of the containment below the water pool would result in even smaller releases due to reactor pool scrubbing.

[redacted]

[redacted]

Figures 3.4 and 3.5 show that the transfer of the RPV water to the containment results in an accumulation of 8 meters of water in the containment. This water in containment would provide further scrubbing of fission products.

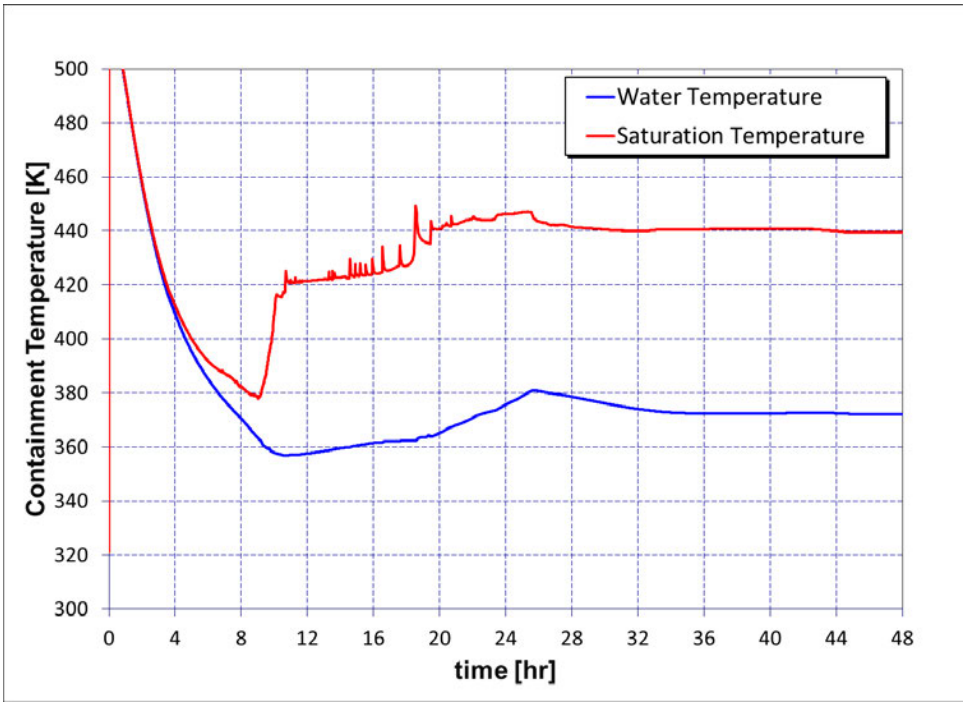

Figure 3.1 Containment Temperature for Scenario LEC-06T

[redacted]

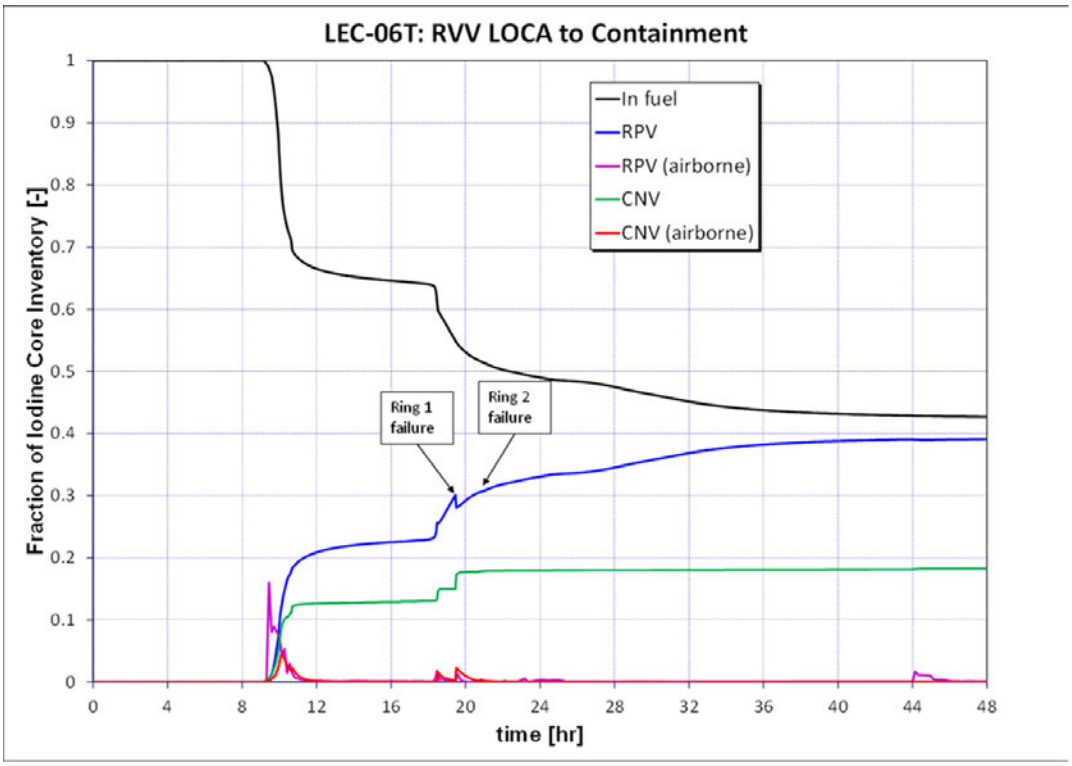

Figure 3.2 Iodine Distribution for Scenario LEC-06T

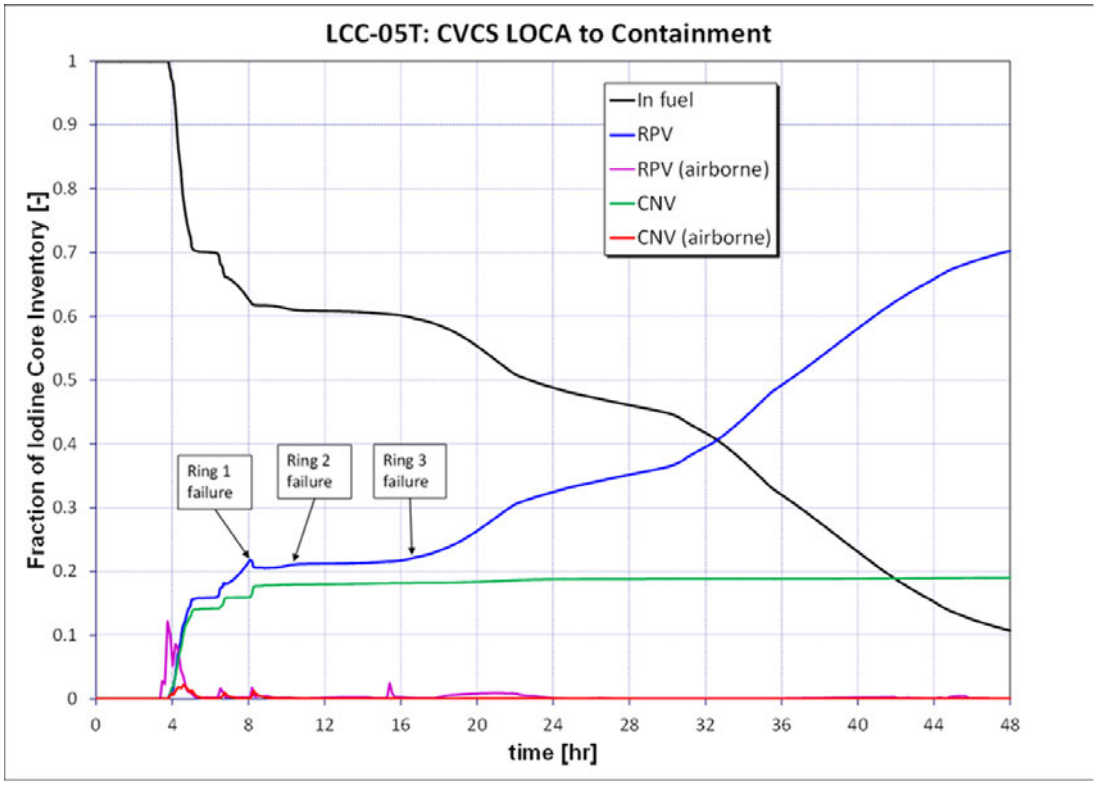

Figure 3.3 Iodine Distribution for Scenario LCC-05T

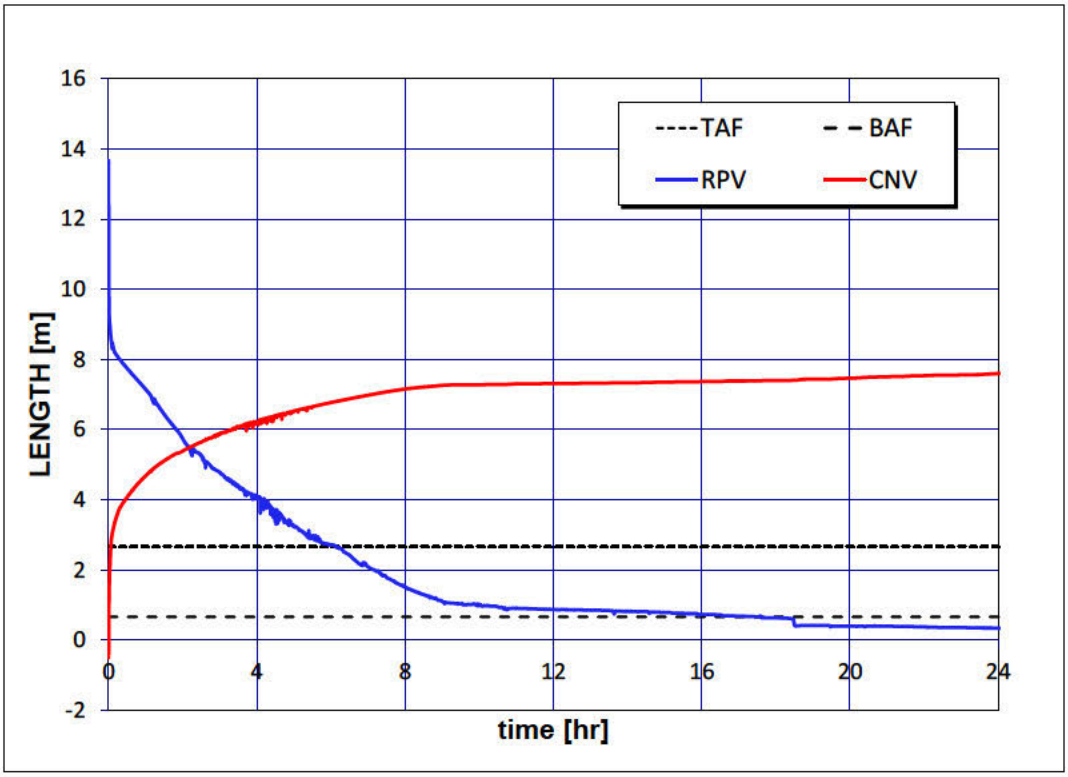

Figure 3.4 Water levels for Scenario LEC-06T

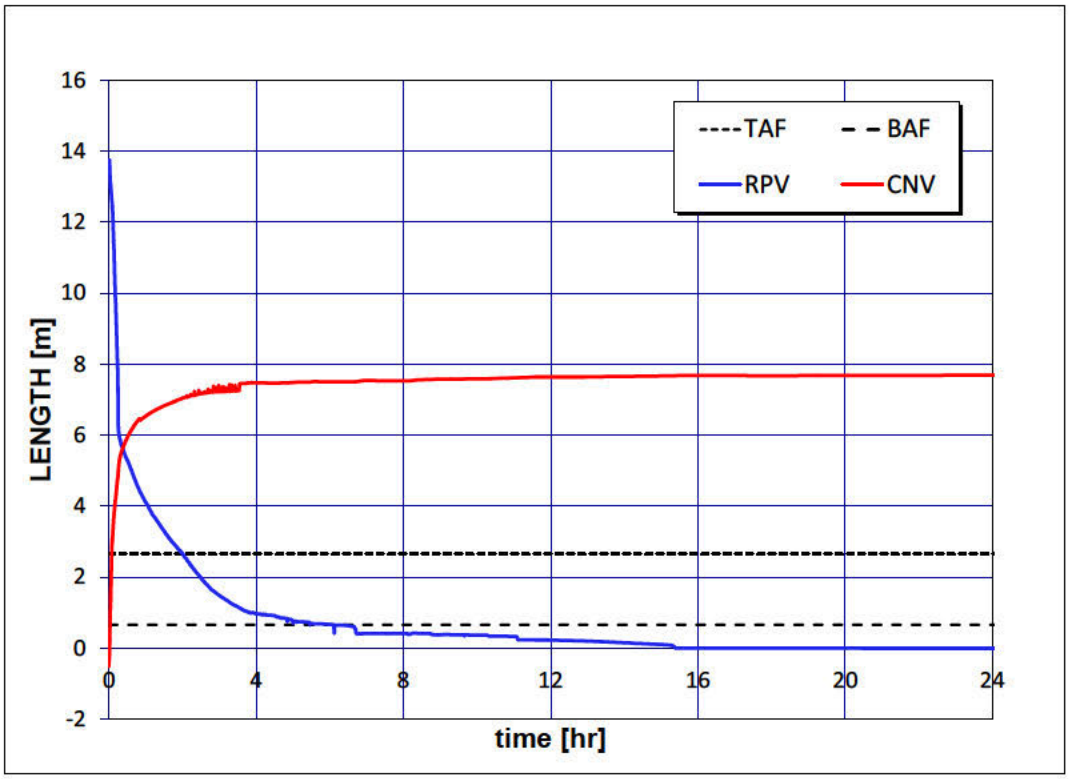

Figure 3.5 Water Levels for Scenario LCC-05T

4.0 REFERENCES

Corradini, M. L. (1988). Vapor Explosions in Light Water Reactors: A Review of Theory and Modeling. *Prog. Nucl. Energy, 22, p. 1-117*.

Corradini, M. L. (2011, July). Evaluation of Dynamic Pressures from Steam Explosions Applied to Advanced Light Water Reactors. *Nuclear Science and Engineering*.

Liu, J. (2005). Evaluation of the Energy Conversion Ratio of Vapor Explosions for the Assessment of Nuclear Reactor Safety. *J. Nucl. Science and Technology, Vol. 42, No. 1, p 28-39*.

U.S. NRC. (1975, October). WASH-1400, Reactor Safety Study.

U.S. NRC. (1984, March). NUREG/CR-3624, A FORTRAN 77 Program and User's Guide for the Generation of Latin Hypercube and Random Samples for Use with Computer Models.

U.S. NRC. (1989, February). NUREG/CR-5030, An Assessment of Steam-Explosion-Induced Containment Failure.

U.S. NRC. (2004, August). NUREG/CR-6849, Analysis of In-Vessel Retention and Ex-Vessel Fuel Coolant Interaction for AP1000.

U.S. NRC. (2018, August). FSCB-18-01, Independent MELCOR Confirmatory Analysis for NuScale Small Modular Reactor, draft.